



This is an *Accepted Manuscript*, which has been through the RSC Publishing peer review process and has been accepted for publication.

Accepted Manuscripts are published online shortly after acceptance, which is prior to technical editing, formatting and proof reading. This free service from RSC Publishing allows authors to make their results available to the community, in citable form, before publication of the edited article. This *Accepted Manuscript* will be replaced by the edited and formatted *Advance Article* as soon as this is available.

To cite this manuscript please use its permanent Digital Object Identifier (DOI®), which is identical for all formats of publication.

More information about *Accepted Manuscripts* can be found in the [Information for Authors](#).

Please note that technical editing may introduce minor changes to the text and/or graphics contained in the manuscript submitted by the author(s) which may alter content, and that the standard [Terms & Conditions](#) and the [ethical guidelines](#) that apply to the journal are still applicable. In no event shall the RSC be held responsible for any errors or omissions in these *Accepted Manuscript* manuscripts or any consequences arising from the use of any information contained in them.

Sensitive and selective colorimetric sensing of Fe³⁺ ion by using *p*-amino salicylic acid dithiocarbamate functionalized gold nanoparticles

Vaibhavkumar N Mehta^a, Suresh Kumar Kailasa^{a*} and Hui-Fen Wu^b

^a*Department of Chemistry, S. V. National Institute of Technology, Surat-395 007, India*

^b*Department of Chemistry, National Sun Yat Sen University, Kaohsiung, 804, Taiwan*

**Corresponding author, Phone: +91-261-2201730; Fax: +91-261-2227334
E-mail: sureshkumarchem@gmail.com; skk@ashd.svnit.ac.in*

Abstract

We have developed a selective and sensitive colorimetric method for determination of Fe^{3+} ion by using *p*-amino salicylic acid dithiocarbamate functionalized gold nanoparticles (DTC-PAS-Au NPs) as colorimetric probes. The DTC-PAS-Au NPs were characterized by FT-IR, ^1H NMR, UV-visible spectrometry, transmission electron microscopy (TEM), dynamic light scattering (DLS) and atomic force microscopic (AFM) techniques, respectively. The DTC-PAS-Au NPs are aggregated rapidly by addition of Fe^{3+} ion, yielding a color change from red to blue. The characteristic surface plasmon resonance (SPR) peak (520 nm) of DTC-PAS-Au NPs was shifted to longer wavelength 700 nm, which confirms the ligand-to-metal charge transfer between DTC-PAS-Au NPs and Fe^{3+} ion. Under the optimal conditions, a good linear relationship (correlation coefficient $R^2 = 0.993$) was obtained between the ratio of the extinction at 700 nm to that at 520 nm and the concentration of Fe^{3+} over the range of 40 - 80 μM , with a detection limit of 14.82 nM. The DTC-PAS-Au NPs acted as colorimetric sensors for the selective detection of Fe^{3+} ions in real samples (blood and urine samples).

Keywords: DTC-PAS-Au NPs, Fe^{3+} ion, UV-visible spectrometry, FT-IR, TEM and DLS

Introduction

Development of novel colorimetric sensors has attracted significant interest for selective and sensitive detection of metal ions in environmental and biological samples.¹⁻⁵ Iron is the most abundant vital transition metal in the plants and human body which plays a significant role in cellular metabolism, and enzymatic catalysis. It acted as a carrier for oxygen and electron transports in hemoglobin and served as a cofactor in many enzymatic reactions.⁶⁻¹⁰ However, the excess amount of Fe^{3+} ion can be caused to damage cellular lipids, nucleic acids and proteins, respectively. Furthermore, the deficiency of Fe^{3+} ion limits oxygen delivery to cells and causes anemia, liver and kidney damages, diabetes, and heart diseases.¹¹⁻¹³ Therefore, the detection of Fe^{3+} ion has become a matter of considerable interest in environmental and biological samples. The conventional Fe^{3+} assays are performed by using several analytical techniques such as inductively coupled-plasma atomic emission spectrometry (ICP-AES),¹⁴ inductively coupled plasma mass spectrometry (ICPMS),¹⁵⁻¹⁶ atomic absorption spectrometry (AAS)¹⁷ and voltametry,¹⁸ respectively. However, these methods are expensive and required tedious sample pretreatment procedures. Therefore, the development of a facile, inexpensive, selective and *in situ* method that allows real-time monitoring of metal species is a great challenge.

In recent years, significant research efforts have been devoted to the design and preparation of Au NPs as promising colorimetric probes for the analysis of wide variety molecules in environmental and biological samples.¹⁹⁻²² The colorimetric sensing approaches are based on their SPR spectral shift by a strong overlap between the plasmon fields of the nearby particles, resulting color change from red to blue.²³⁻²⁵ This fact due to the strong interactions between tailored organic molecules on Au NPs and target analytes,

which allows Au NPs-induced aggregation with analytes. Therefore, surface functionalization of Au NPs plays a crucial role in increasing their analytical applicability for detection of trace analytes with high selectivity and sensitivity.^{24,26} In this connection, dithiocarbamate molecular assembly on Au NPs have shown significant interest in nanoanalytical sciences due to their easy preparation and very less interatomic distance between two sulfur atoms which facilitate a strong binding with NPs surface.²⁷ As a result, dithiocarbamate derivatives functionalized Au NPs have been used as selective probes for detection of biomolecules,²⁸ anions²⁹ and cations,³⁰⁻³¹ respectively.

In this paper, we explore the utility of DTC-PAS-Au NPs as colorimetric probe for detection of Fe^{3+} in environmental and biological samples. The DTC-PAS-Au NPs aggregated rapidly by addition of Fe^{3+} ion, resulting a color change from red to blue, which induces by ligand-to-metal charge transfer between $-\text{OH}$ and $-\text{COOH}$ groups of DTC-PAS-Au NPs and Fe^{3+} (Scheme 1). This colorimetric probe opens up new possibilities for developing analytical methods for the monitoring of Fe^{3+} in biological samples without any sample pretreatment procedure.

Experimental

Chemicals and materials

Hydrogen tetrachloroaurate hydrate ($\text{HAuCl}_4 \cdot x\text{H}_2\text{O}$), *p*-amino salicylic acid, metal salts ($\text{Zn}(\text{NO}_3)_2 \cdot 6\text{H}_2\text{O}$, $\text{Mn}(\text{NO}_3)_2 \cdot 4\text{H}_2\text{O}$, $\text{Co}(\text{NO}_3)_2 \cdot 6\text{H}_2\text{O}$, $\text{Pb}(\text{NO}_3)_2$, $\text{Cd}(\text{NO}_3)_2 \cdot 4\text{H}_2\text{O}$, $\text{Cu}(\text{NO}_3)_2 \cdot 3\text{H}_2\text{O}$, $\text{Hg}(\text{NO}_3)_2 \cdot \text{H}_2\text{O}$, $\text{FeCl}_2 \cdot 4\text{H}_2\text{O}$, $\text{Mg}(\text{NO}_3)_2 \cdot 6\text{H}_2\text{O}$, $\text{NiSO}_4 \cdot 6\text{H}_2\text{O}$, $\text{FeCl}_3 \cdot 6\text{H}_2\text{O}$), phosphate-buffered saline (PBS), Tris-HCl (Tris) and sodium acetate (NaAc) were obtained from Sigma-Aldrich, USA. Dimethyl formaldehyde (DMF) and

carbon disulfide were purchased from Merck Ltd., India. Trisodium citrate dihydrate was purchased from SD Fine Chemicals Ltd., India. Blood and urine samples were collected from healthy volunteers. All chemicals were of analytical grade and used without further purification. Milli-Q-purified water was used for the sample preparations. *Caution:* Blood samples were obtained from Shivam Pathological Laboratory, Surat, Gujarat, India, which is approved by All India Institute of Medical Sciences, New Delhi, India. The blood samples were collected by confirming informed consent. All experiments were performed in compliance with the relevant laws and institutional guidelines, and this study was also approved by the Institute Research Committee, S. V. National Institute of Technology, Surat, Gujarat, India.

Synthesis of DTC-PAS-Au NPs

Dithiocarbamate derivative of *p*-amino salicylic acid was synthesized according to the reported method in the literature.³² Briefly, equimolar mixture of *p*-amino salicylic acid and CS₂ in ethanolic KOH (50 mL, 5%) and DMF (50 mL) was warmed at 45 °C for 30 minutes and then cooled. The reaction mixture was acidified with dilute AcOH. The resulting solid product was filtered and recrystallized from methanol as orange needles. Citrate-capped Au NPs were prepared according to Frens' method.³³ Briefly, 100 mL of 1 mM HAuCl₄ was taken into a round-bottom flask and then boiled under vigorous stirring for 20 min. To this, 38.8 mM of trisodium citrate (10 mL) was added rapidly into the reaction flask and the mixture was stirred for another 15 min. The color of solution was changed from pale yellow to deep red, confirming the formation of Au NPs. The concentration of the Au NPs was calculated according to Beer's law by using an extinction coefficient of ca. $10^8 \text{ M}^{-1} \text{ cm}^{-1}$ at 520 nm³⁴ and found to be 12.28 nM. To obtain

DTC-PAS-Au NPs, 25 μL of 1 mM DTC-PAS was added into 20 mL of Au NPs and then stirred for 1 h at room temperature (Supporting Information of Figure S1). The resulting Au NPs solution was used for the colorimetric sensing of Fe^{3+} in biological samples.

Detection of Fe^{3+} using DTC-PAS-Au NPs

The stock solution of ferric chloride (1 mM) was prepared by dissolving ferric chloride in deionised water. For the detection of Fe^{3+} by using the DTC-PAS-Au NPs, 100 μL of different concentrations of Fe^{3+} solutions were added separately into a 1.5 mL of DTC-PAS-Au NPs solution, and the pH was adjusted to 6.0 by using PBS buffer. The sample vials were vortexed 30 s and the color of the solution was changed from red to purple then blue. The resulting Au NPs UV-visible spectral changes were measured by using a Maya Pro 2000 spectrophotometer. Furthermore, we also evaluated the stability of Au NPs before and after functionalization. It was noticed that citrate modified Au NPs are stable for 2 months and well agreed with the literature.³⁵ At the same time, DTC-PAS-Au NPs are stable for 3-4 weeks after that there is a slightly color change due to the electrostatic interactions and hydrogen bonding formation between DTC-PAS-Au NPs. However, the rapid color change of DTC-PAS-Au NPs solution (red to blue) was attributed to the DTC-PAS-Au NPs aggregation induced by Fe^{3+} ion (10 - 100 μM).

Instrumentation

UV-visible spectra were measured with a Maya Pro 2000 spectrophotometer (Ocean Optics, USA) at room temperature. ^1H NMR spectra were recorded on a Varian 400 MHz instrument. Fourier transform infrared (FT-IR) spectra were recorded on a

Perkin Elmer (FT-IR spectrum BX, Germany). Transmission electron microscopy (TEM) images were taken on a Tecnai 20 (Philips, Holland) at an acceleration voltage of 100 kV. DLS measurements were performed by using Zetasizer Nano ZS90 (Malvern, UK).

Results and discussion

Characterization of DTC-PAS-Au NPs

The synthesized DTC-PAS-Au NPs were characterized by spectroscopic (UV-visible, FT-IR and $^1\text{H NMR}$) and microscopic (TEM, AFM and DLS) techniques. Figure 1 shows the UV-visible spectra of bare Au NPs and DTC-PAS-Au NPs. It can be noticed that the characteristic SPR peak (520 nm) of Au NPs was slightly red-shift and the peak intensity was little decreased after functionalization of DTC-PAS molecules onto the surfaces of Au NPs. Supporting Information of Figure S2 illustrates the typical FT-IR spectra of pure *p*-amino salicylic acid, DTC-PAS and DTC-PAS-Au NPs. FT-IR spectrum of pure *p*-amino salicylic acid shows the two characteristic bands at 3495 and 3388 cm^{-1} corresponding to -N-H asymmetric and symmetric stretching modes, respectively. The strongest absorption peak at 1644 cm^{-1} belongs to C=O stretching mode of COOH group in PAS. Supporting Information of Figure S2b shows the FT-IR spectrum of DTC-PAS. In this spectrum, C-S, -S-H and CS-NH groups stretching vibrations were observed at 1100, 2561 and 1228 cm^{-1} , respectively. Importantly, it can be noticed that the mercapto group (-SH) stretching and bending modes were not observed at 2543–2550 cm^{-1} in the spectrum of DTC-PAS-Au NPs, conforming the new bond formation between DTC-PAS and surfaces of Au NPs (Supporting Information of Figure S2c). These results revealed that DTC-PAS molecules were successfully attached

onto the surfaces of Au NPs *via* a simple “zero-length” covalent coupling.

Supporting Information of Figure S3 represents ^1H NMR spectra of pure *p*-amino salicylic acid, DTC-PAS and DTC-PAS-Au NPs. ^1H NMR spectrum of pure *p*-amino salicylic acid shows the multiplet peaks 6.0 – 7.0 ppm, which are assigned to aromatic protons of PAS. The peaks at 11.37 (singlet) ppm and 12.53 (singlet) ppm corresponded to –OH protons of PAS. The peak at 5.98 (doublet) ppm corresponds to –NH₂ protons of PAS. The appearance of new peak at ~1.19 ppm confirms the proton peak of mercapto (–SH) group of DTC-PAS (Supporting Information of Figure S3b). However, the proton peaks of DTC-PAS-Au NPs were disappeared in the spectrum of DTC-PAS-Au NPs, which confirms the change in their chemical environment and the presence of water molecules in the DTC-PAS-Au NPs (Supporting Information of Figure S3c).

It is well known that the average size of NPs can be estimated by calculating the mean hydrodynamic diameter in response from the autocorrelation function of the intensity of light scattered from the particles *via* Brownian motion.³⁹ Figure 2 a-b shows the DLS data of bare Au NPs and DTC-PAS-Au NPs. It is observed that the bare Au NPs are monodispersed with an average hydrodynamic diameter of ~10 nm. However, the hydrodynamic diameter of Au NPs was increased to ~43 nm due to surface modifications of Au NPs with DTC-PAS (Figure 2b). Since, DTC-PAS molecules are bulky and covalently attached onto the surfaces of Au NPs, resulting to increase their hydrodynamic diameter.⁴⁰ Figure 3a shows the TEM image of DTC-PAS-Au NPs and the functionalized Au NPs are well dispersed with an average size of ~40 nm, which is well agreed with DLS data. The DTC-PAS-Au NPs are in spherical shape. Furthermore, we also studied the AFM of DTC-PAS-Au NPs (Figure 4a). This result indicates that DTC-PAS-Au NPs

are not aggregated and can be used as colorimetric probes for sensing of metal ions.

DTC-PAS-Au NPs as colorimetric probes sensing of Fe³⁺ ion

To investigate the analytical application of DTC-PAS-Au NPs as sensors for metal ions, various metal ions (Cu²⁺, Fe²⁺, Mg²⁺, Mn²⁺, Hg²⁺, Zn²⁺, Ni²⁺, Co²⁺, Pb²⁺, Cd²⁺ and Fe³⁺, 500 μM) were added into DTC-PAS-Au NPs solutions (Figure 5a). It can be observed that there is a drastic decrease in the SPR peak of DTC-PAS-Au NPs at 520 nm, and a new absorption peak is generated at 700 nm with only addition of Fe³⁺ ions, which clearly confirms the DTC-PAS-Au NPs-induced aggregation with Fe³⁺ ion (Figure 5a). This newly generated peak around 700 nm is attributed due to the coordinate covalent bonds between –OH and –COOH groups of DTC-PAS-Au NPs and Fe³⁺, which leads to ligand-to-metal charge transfer. As a result, the color of DTC-PAS-Au NPs solution was changed from red to blue, which can be observed with naked eye (Figure 5b). This result strongly indicates that Fe³⁺ ion has shown high ability to interact with –OH and –COOH groups of DTC-PAS-Au NPs surfaces, resulting DTC-PAS-Au NPs-induced aggregations through electric dipole–dipole interactions and coupling between the plasmon of neighboring nanoparticles.²⁶ Supporting Information of Figure S4 represents the colorimetric sensing ability of DTC-PAS-Au NPs with other metal species was expressed by the ratio of absorption at 700 nm to that at 520 nm ($A_{700\text{ nm}/520\text{ nm}}$), indicating that DTC-PAS-Au NPs showed high selectivity towards Fe³⁺ than the other metal species.

Sensing mechanism for Fe³⁺ ion

As shown in Supporting Information of Figure S1, *p*-amino salicylic acid contains amino (-NH₂), phenolic (-OH) and carboxylic acid groups (-COOH). It is well known that -NH₂ group of PAS is already involved in the preparation of DTC-PAS followed by their molecular assembly onto the surfaces of Au NPs *via* thiolate linkage (-NH-CS₂-Au NPs), which confirms the blocking of free -NH₂ groups to avoid the complex formation DTC-PAS-Au NPs with the divalent metal ions (Fe²⁺, Zn²⁺, Cd²⁺).³⁶ After functionalization of DTC-PAS with Au NPs, only -OH and -COOH are available to form complex with Fe³⁺ ion. These groups have negative charges when the pH is >4. Since, the pK_{a1}, and pK_{a2} values of PAS are 1.79 and 3.92 and these groups are effectively coordinate with Fe³⁺ ion, respectively.³⁷⁻³⁸ Therefore, these negatively charged groups (-O⁻ and -COO⁻) can be effectively make complex with Fe³⁺, which can induce a higher degree of DTC-PAS-Au NPs aggregations.

Effect of pH

We investigated the effect of buffer pH on the colorimetric sensing ability of DTC-PAS-Au NPs for Fe³⁺ ion detection. Figure 6 shows the intensities of the extinction ratios ($A_{700\text{nm}}/A_{520\text{nm}}$) of DTC-PAS-Au NPs upon the addition of Fe³⁺ ion at PBS, Tris and NaAc buffer systems pH from 2 – 10. Even though the intensities of extinction ratios of DTC-PAS-Au NPs-Fe³⁺ solutions are good by using three buffers at low pH 2-4, but this pH range is not suitable for colorimetric sensing of Au NPs. Since, Au NPs surfaces can be neutralized at low pH (<4), which allows Au NPs self aggregation without addition of analytes. As shown in Figure 6, the extinction ratio ($A_{700\text{nm}}/A_{520\text{nm}}$) of DTC-PAS-Au NPs induced aggregation with Fe³⁺ ion had reached its maximum at pH 6.0. This may be because DTC-PAS-Au NPs have negative charges when the pH value is higher than 4.0,

and this allows a high degree of DTC-PAS-Au NPs-induced aggregations with Fe^{3+} ion. Therefore, a pH of 6.0 of the PBS buffer solution was selected.

Confirmation of DTC-PAS-Au NPs-induced aggregations with Fe^{3+} ion by DLS, TEM and AFM

In order to confirm the DTC-PAS-Au NPs-induced aggregations with Fe^{3+} ion, we studied DLS, TEM and AFM techniques. As shown in Figure 2c, the hydrodynamic diameter of DTC-PAS-Au NPs was drastically increased to ~ 412 nm by the addition of Fe^{3+} ion, yielding the DTC-PAS-Au NP aggregation *via* the complex formation between DTC-PAS-Au NPs and Fe^{3+} ion. Figure 3b shows the TEM image of DTC-PAS-Au NPs induced aggregations with Fe^{3+} ion. It can be noticed that the morphology and sizes of DTC-PAS-Au NPs were greatly influenced by the addition of Fe^{3+} , which results to change their state from monodisperse to polydisperse. Furthermore, the aggregation of DTC-PAS-Au NPs with Fe^{3+} was also verified by using AFM technique. Figure 4b shows the AFM image of DTC-PAS-Au NPs induced aggregation with Fe^{3+} ion at three dimensions. This result confirms the DTC-PAS-Au NPs induced aggregations with Fe^{3+} ion.

Quantification of Fe^{3+} by using DTC-PAS-Au NPs as colorimetric probes

The potentiality of DTC-PAS-Au NPs based UV-visible spectrometric method was demonstrated for the quantification of Fe^{3+} in aqueous samples as model to analytical problem. At the optimized conditions, various concentrations (10 to 100 μM) of Fe^{3+} were added into DTC-PAS-Au NPs solution separately and their UV-visible spectra were measured. As shown in Figure 7b, the color of Au NPs solutions are gradually changed from red to purple and then blue upon increasing concentration of Fe^{3+} ion, which could

be observed by the naked eye. It can be observed that the increasing concentrations of Fe^{3+} ion, the SPR peak of Au NPs at 520 nm decreased gradually, along with the increased a new SPR peak at 700 nm (Figure 7a). Furthermore, a calibration graph was constructed between UV–vis extinction ratio ($A_{700\text{nm}}/A_{520\text{nm}}$) and concentration of Fe^{3+} ions ranging from 40 to 80 μM ($y = 1.923x - 2.846$), which can be used for the quantification of Fe^{3+} with a correlation coefficient of 0.993 (Figure 8), and the detection limit (LOD) is 14.82 nM, respectively. In addition, we also compared the sensitivity of present method with the reported NPs-based UV-visible and fluorescence methods for detection of Fe^{3+} ion (Table 1). It indicates that the present method showed higher sensitivity than that of the NPs-based UV-visible^{41-42,44-45} and fluorescence^{43,46-47} methods. Therefore, this analytical system exploits the advantages of DTC-PAS-Au NPs as colorimetric sensors for the detection of Fe^{3+} by using UV-visible spectrometry.

Interference studies

To demonstrate the selectivity of DTC-PAS-Au NPs for Fe^{3+} ion, competitive experiments were carried out in the presence of other metal ions (Cu^{2+} , Fe^{2+} , Mg^{2+} , Mn^{2+} , Hg^{2+} , Zn^{2+} , Ni^{2+} , Co^{2+} , Pb^{2+} and Cd^{2+} , 100 μM) for detection of Fe^{3+} ion. It can be noticed that the SPR peak shift caused only at the mixture of metal ions solution that contained Fe^{3+} ion, resulting a visible color change from red to blue, which is just like as solely addition of Fe^{3+} ion into Au NPs solution (Supporting Information of Figure S5). This result clearly indicates that this method was free from interference of other metal ions, which should be noted for practical application to Fe^{3+} assays in real samples.

Application of DTC-PAS-Au NPs for the analysis of Fe³⁺ ion in blood and urine samples

The proposed DTC-PAS-Au NPs sensor has been applied to detect Fe³⁺ ion in blood and urine samples. To this, human serum and urine samples were collected from healthy adult volunteers. The collected blood samples were centrifuged at 5000 rpm for 15 min. The collected supernatant (serum) were diluted 100-fold with ultrapure water and used for further analysis. Urine sample were filtered through a 0.45 μm membrane and diluted 100-fold with ultrapure water. The above blood and urine samples were spiked with different known concentrations of Fe³⁺ (10, 50 and 100 μM) and then the concentration of Fe³⁺ ion was estimated by the aforesaid procedure. Supporting Information of Figure S6 shows the UV-visible spectra for the spiked blood serum and urine samples at three different concentrations (10, 50 and 100 μM). The amount of Fe³⁺ ion was estimated by using the present method and the obtained data were shown in Table 2. This result indicates that this method showed good recoveries in the range of 95% - 98.76 % and 92.2% - 98.27% for blood and urine samples, with relative standard deviation (%RSD) values in the range of 0.88% - 1.17 % and 0.90% - 1.21% for blood and urine samples, respectively. This indicates the present method exhibits good precision for the analysis of Fe³⁺ in blood and urine samples. In order to estimate the accuracy of the present method, we studied intra- and inter-day precision and accuracy of the method for the analysis of Fe³⁺ ion in spiked aqueous and urine samples. As shown in Table 3, this method shows good precision (RSD < 4.35%) and accuracy (-0.0462 to +0.0236) for the analysis of Fe³⁺ ion in spiked aqueous urine samples. Supporting Information of Figure S7 shows the measured UV-visible spectra DTC-PAS-Au NPs

upon the addition of Fe^{3+} ion ($100 \mu\text{M}$) at intra- and inter- day. These results indicate that the reliability of DTC-PAS-Au NPs as ideal colorimetric probes for Fe^{3+} determination in real samples.

Conclusions

In summary, we present a simple, selective and sensitive DTC-PAS-Au NPs-based UV-visible method for on-site, and real-time detection of Fe^{3+} in biological samples. The Fe^{3+} ion-induced aggregates of DTC-PAS-Au NPs were characterized by UV-visible, DLS, TEM and AFM, respectively. The extinction ratio $A_{700\text{nm}}/A_{520\text{nm}}$ is linear with the concentration of Fe^{3+} ranging from $40 \mu\text{M}$ to $80 \mu\text{M}$, which proves a sensitive detection of Fe^{3+} ion with a detection limit of 14.82 nM . This method was free from the interference of other metal ions and exhibited good precision and accuracy for detection of Fe^{3+} ion in aqueous and urine samples. Therefore, DTC-PAS-Au NPs can be utilized as a novel colorimetric sensor for the rapid, selective and real-time *in situ* detection of Fe^{3+} in biological samples, and it would open great prospective for practical applications to Fe^{3+} ion assays in environmental and biological samples.

Acknowledgement

We gratefully acknowledge the Director, SVNIT for providing all the facilities to carry out this work. We also thank Department of Science and Technology, India for providing UV-visible spectrophotometer for this analysis. We would like to thank Mr. Vikas Patel, SICART, Anand, V. V. Nagar for their assistance in TEM data. The authors thank Shivam Pathological Laboratory, Surat, Gujarat, India for providing blood samples.

References

1. A. P. de silva, H. Q. N. Gunaratne, T. Gunnlaugsson, A. J. M. Huxley, C. P. McCoy, J. T. Rademacher and T. E. Rice, *Chem. Rev.*, 1997, **97**, 1515.
2. K. Rurack and U. R. Genger, *Chem. Soc. Rev.*, 2002, **31**, 116.
3. V. Amendola, L. Fabbrizzi, F. Forti, M. Licchelli, C. Mangano, P. Pallavicini, A. Poggi, D. Sacchi and A. Taglieti, *Coord. Chem. Rev.*, 2006, **250**, 273.
4. D. T. Quang and J. S. Kim, *Chem. Rev.*, 2010, **110**, 6280.
5. R.H. Holm, P. Kennepohl and E.I. Solomon, *Chem. Rev.*, 1996, **96**, 2239.
6. R. Meneghini, *Free Radical Biol. Med.*, 1997, **23**, 783.
7. R. S. Eisenstein, *Annu. Rev. Nutr.*, 2000, **20**, 627.
8. T. A. Rouault, *Nat. Chem. Biol.*, 2006, **2**, 406.
9. J. A. Cowan, *Inorganic Biochemistry: An Introduction*, Wiley-VCH, New York, 1997, 167.
10. C. Brugnara, *Clin. Chem.*, 2003, **49**, 1573.
11. J. D. Haas and T. Brownlie IV, *J. Nutr.*, 2001, **131**, 676.
12. O. K. Fix and K. V. Kowdley, *Minerva Med.*, 2008, **99**, 605.
13. P. Aisen, M. W. Resnick and E. A. Leibold, *Curr. Opin. Chem. Biol.*, 1999, **3**, 200.
14. K. Pomazal, C. Prohaska, I. Steffan, G. Reich and J. F. K. Huber, *Analyst*, 1999, **124**, 657.
15. M. E. C. Busto, M. M. Bayon, E. B. Gonzalez, J. Meija and A. S. Medel, *Anal. Chem.*, 2005, **77**, 5615.
16. G. L. Arnold, S. Weyer and A. D. Anbar, *Anal. Chem.*, 2004, **76**, 322.
17. J. E. T. Andersen, *Analyst*, 2005, **130**, 385.

18. C. M. G. van den Berg, *Anal. Chem.*, 2006, **78**, 156.
19. D. C. Hone, A. H. Haines and D. A. Russell, *Langmuir*, 2003, **19**, 7141.
20. S. H. Wu, Y. S. Wu and C. H. Chen, *Anal. Chem.*, 2008, **80**, 6560.
21. J. S. Lee, M. S. Han and C. A. Mirkin, *Angew. Chem., Int. Ed.*, 2007, **46**, 4093.
22. D. Li, A. Wieckowska and I. Willner, *Angew. Chem., Int. Ed.*, 2008, **47**, 3927.
23. S. Kubo, A. Diaz, Y. Tang, T. S. Mayer, I. C. Khoo and T. E. Mallouk, *Nano Lett.*, 2007, **7**, 3418.
24. M. C. Daniel and D. Astruc, *Chem. Rev.*, 2004, **104**, 293.
25. H. Li, Q. Zheng and C. Han, *Analyst*, 2010, **135**, 1360.
26. H. Cao, M. Wei, Z. Chen and Y. Huang, *Analyst*, 2013, **138**, 2420.
27. P. Morf, F. Raimondi, H. G. Nothofer, B. Schnyder, A. Yasuda, J. M. Wessels and T. A. Jung, *Langmuir*, 2006, **22**, 658.
28. S. K. Kailasa and H. F. Wu, *Analyst*, 2012, **137**, 1629.
29. A. Pandya, K. V. Joshi, N. R. Modi and S. K. Menon, *Sens. Actuators, B*, 2012, **168**, 54.
30. V. N. Mehta, A. K. Mungara and S. K. Kailasa, *Anal. Methods*, 2013, **5**, 1818.
31. V. N. Mehta, A. K. Mungara and S. K. Kailasa, *Ind. Eng. Chem. Res.*, 2013, **52**, 4414.
32. M. S. I. T. Makki, R. M. Abdel-Rahman, H. M. Faidallah, and K. A. Khan, *J. Chem.*, 2013.
33. G. Frens, *Nat. Phys. Sci.*, 1973, 20.
34. C. C. Huang and H. T. Chang, *Chem. Commun.*, 2007, **12**, 1215.

35. S. H. Brewer, W. R. Glomm, M. C. Johnson, M. K. Knag and S. Franzen, *Langmuir*, 2005, **21**, 9303.
36. L. Qi, Y. Shang and F. Wu, *Microchim. Acta*, 2012, **178**, 221.
37. W. A. E. McBryde, J. L. Rohr, J. S. Penciner and J. A. Page, *Can. J. Chem.*, 1970, **48**, 2574.
38. X. X. Ou, X. Quan, S. Chen, F. J. Zhang and Y. Z. Zhao, *J. Photochem. Photobiol., A*, 2008, **197**, 382.
39. X. Liu, Q. Dai, L. Austin, J. Coutts, G. Knowles, J. Zou, H. Chen and Q. Huo, *J. Am. Chem. Soc.*, 2008, **130**, 2780.
40. Q. Wang, L. Yang, X. Yang, K. Wang and J. Liu, *Analyst*, 2013, **138**, 5146.
41. S. P. Wu, Y. P. Chen and Y.M. Sung, *Analyst*, 2011, **136**, 1887.
42. S. K. Tripathy, J. Y. Woo and C. S. Han, *Sens. Actuators, B*, 2013, **181**, 114.
43. J. A. Ho, H. C. Chang and W. T. Su, *Anal. Chem.*, 2012, **84**, 3246.
44. J. Zhan, L. Wen, F. Miao, D. Tian, X. Zhu and H. Li, *New J. Chem.*, 2012, **36**, 656.
45. A. Pandya, P. G. Sutariya, A. Lodha and S. K. Menon, *Nanoscale*, 2013, **5**, 2364.
46. K. Qu, J. Wang, J. Ren and X. Qu, *Chem. Eur. J.*, 2013, **19**, 7243.
47. T. Lai, E. Zheng, L. Chen, X. Wang, L. Kong, C. You, Y. Ruan and X. Weng, *Nanoscale*, 2013, **5**, 8015.

Figure captions

Scheme 1. Schematic representation for colorimetric sensing of Fe^{3+} by using DTC-PAS-Au NPs as colorimetric probes.

Figure 1. UV-visible spectra of (a) bare Au NPs and (b) DTC-PAS-Au NPs. Inset picture show bare Au NPs and DTC-PAS-Au NPs.

Figure 2. DLS of (a) bare Au NPs (b) DTC-PAS-Au NPs and (c) DTC-PAS-Au NPs induced aggregations with Fe^{3+} ion.

Figure 3. TEM images of (a) DTC-PAS-Au NPs and (b) DTC-PAS-Au NPs induced aggregations with Fe^{3+} ion.

Figure 4. AFM images of (a) DTC-PAS-Au NPs and (b) DTC-PAS-Au NPs induced aggregations with Fe^{3+} ion.

Figure 5. (a) UV-visible absorption spectra of DTC-PAS-Au NPs upon the addition of different metal ions (Cd^{2+} , Co^{2+} , Cu^{2+} , Fe^{2+} , Fe^{3+} , Hg^{2+} , Mg^{2+} , Mn^{2+} , Ni^{2+} , Pb^{2+} , Zn^{2+}) **(b)** Photographic images of DTC-PAS-Au NPs in the presence of various metal ions.

Figure 6. The extinction ratio ($A_{700\text{nm}}/A_{520\text{nm}}$) of DTC-PAS-Au NPs induced aggregations with Fe^{3+} ion by using different buffers (PBS, Tris and NaAc) in the pH range of 2 - 10.

Figure 7. (a) UV-visible spectra of DTC-PAS-Au NPs solutions with increasing concentrations of Fe^{3+} in the range of 10 μM - 100 μM . **(b)** Visual color change of DTC-PAS-Au NPs with different concentrations of Fe^{3+} ranging from 10 μM to 100 μM .

Figure 8. Calibration graph was constructed in response to the UV-visible extinction of DTC-PAC-Au NPs solution upon the addition of Fe^{3+} ion (40 μM – 80 μM).

Table 1. Comparison of DTC-PAS-Au NPs as colorimetric sensor for the detection of Fe³⁺ with the reported methods.

Nanoparticles	Capping agent	Size (nm)	LOD (M)	Detection method	Reference
Au NPs	Pyrophosphate	15	5.6×10^{-6}	UV-visible	[41]
Au NPs	-	-	50 ppm	UV-visible	[42]
Au NCs	<i>L</i> -3,4-dihydroxyphenylalanine	2-6	3.5×10^{-6}	Fluorescence	[43]
Ag NPs	Pyridyl-appended calix[4]arene	10	125×10^{-6}	UV-visible	[44]
Ag NPs	p-STEC ₄	52	9.4×10^{-9}	UV-visible	[45]
Carbon dots	-	3.8	0.32×10^{-6}	Fluorescence	[46]
Polymer dots	-	1-4	-	Fluorescence	[47]
Au NPs	DTC-PAS	10	14.82×10^{-9}	UV-visible	Present study

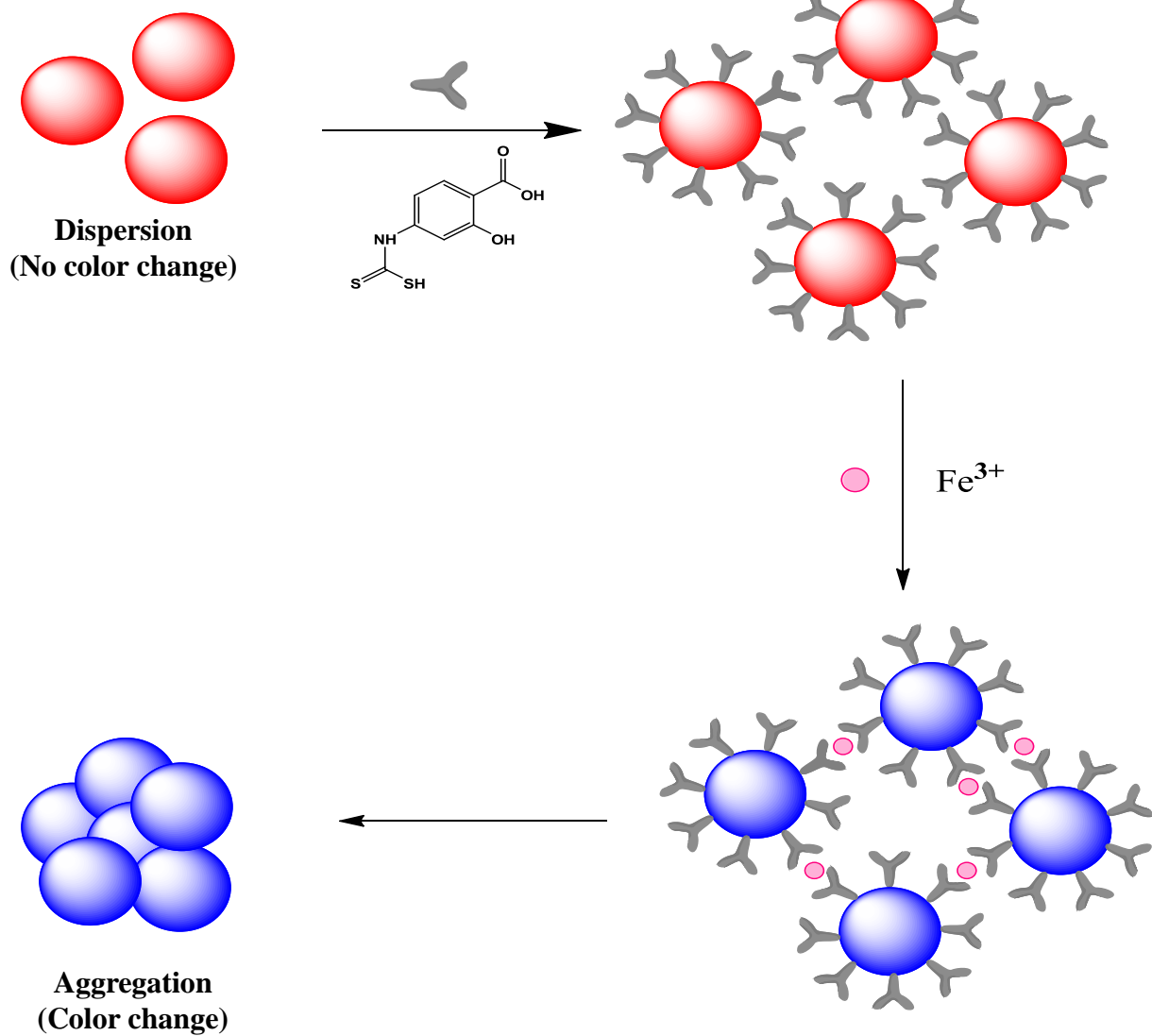
Table 2. DTC-PAS-Au NPs as colorimetric sensor for the analysis of Fe³⁺ in spiked blood and urine samples.

Sample	Added (μM)	Found (μM)	Recovery (%)	RSD (%) (n=3)
Blood sample	10	9.50	95.00	1.17
	50	49.03	98.06	1.18
	100	98.76	98.76	0.88
Urine sample	10	9.22	92.20	1.21
	50	47.48	94.96	1.02
	100	98.27	98.27	0.90

Table 3. Precision and accuracy of present method for the analysis of Fe³⁺ in spiked aqueous and urine samples.

Sample	Known concentration (μM)	Intra-day			Inter-day		
		Found concentration (μM) ^a	R.S.D. (%) ^b	Accuracy ^c	Found concentration (μM) ^a	R.S.D. (%) ^b	Accuracy ^c
Spiked water	100	98.32 ± 0.0285	3.00	-0.0168	98.65±0.0251	2.85	-0.0135
	50	49.08±0.0115	4.35	-0.0184	50.81±0.0101	4.29	+0.0162
Spiked urine	100	101.25±0.044	3.95	+0.0125	97.39±0.0416	3.70	-0.0261
	50	47.69±0.0098	4.31	-0.0462	51.18±0.0105	4.05	+0.0236

^aMean ± standard deviation (n = 3).^bRelative standard deviation.^cAccuracy was calculated from (found concentration – known concentration) / known concentration.



Scheme 1

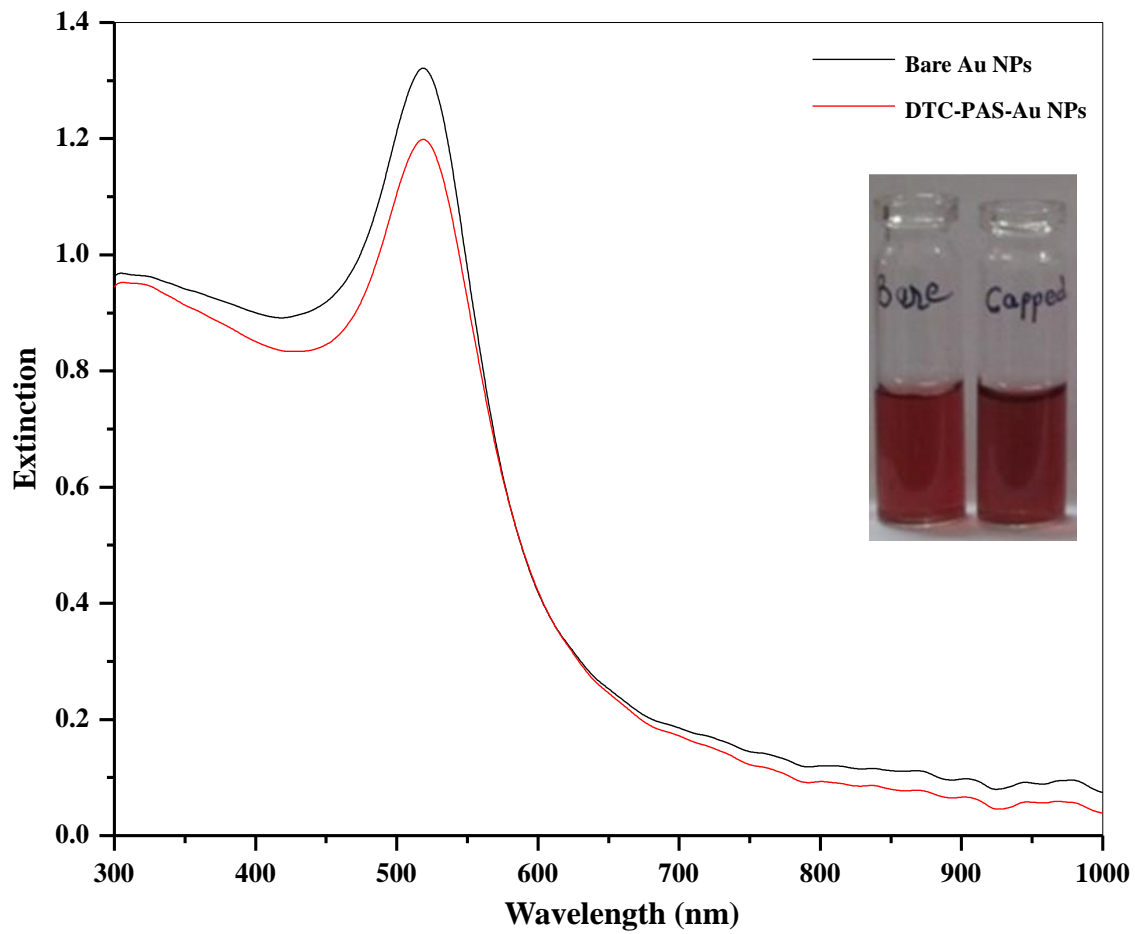


Figure 1

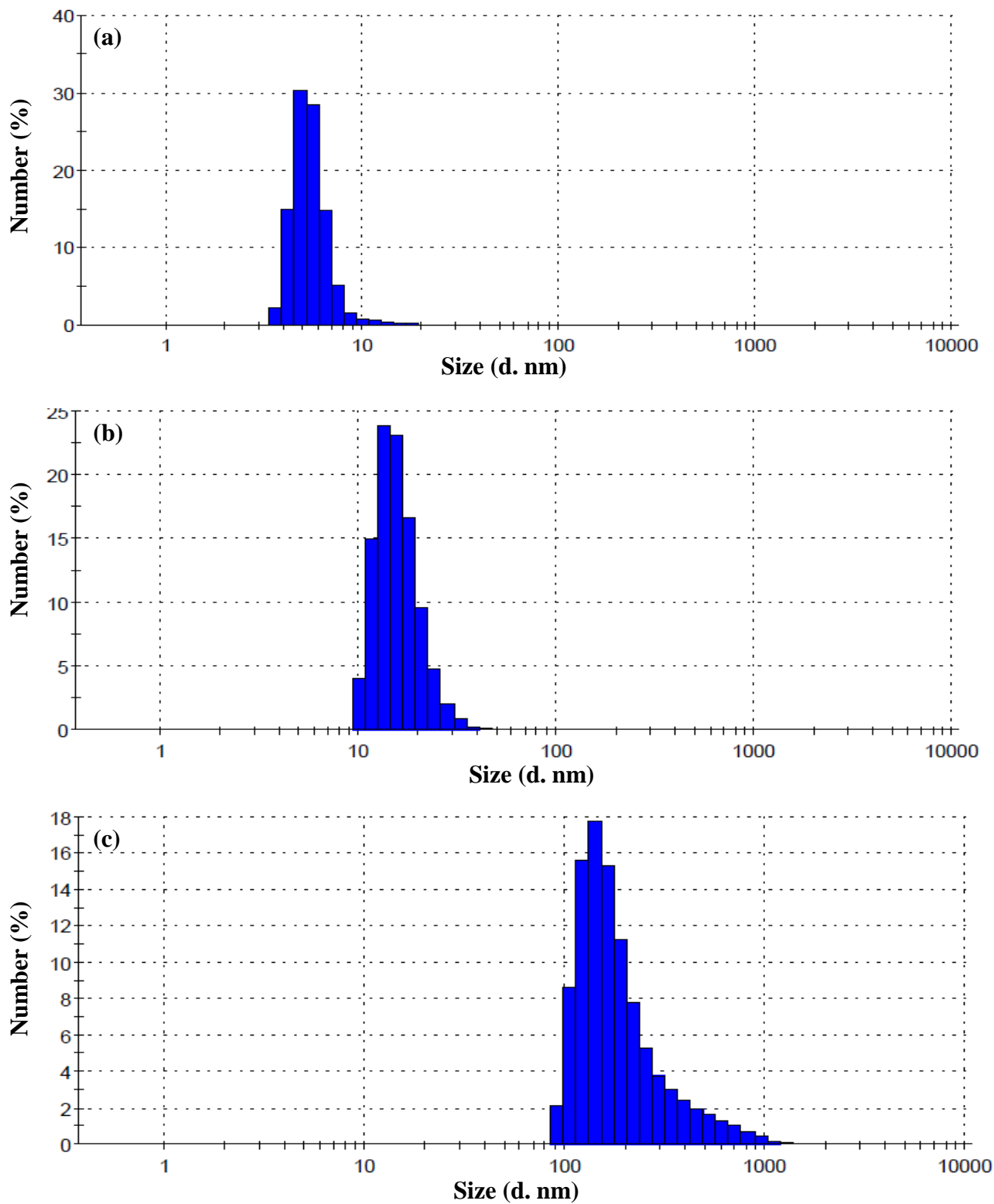


Figure 2

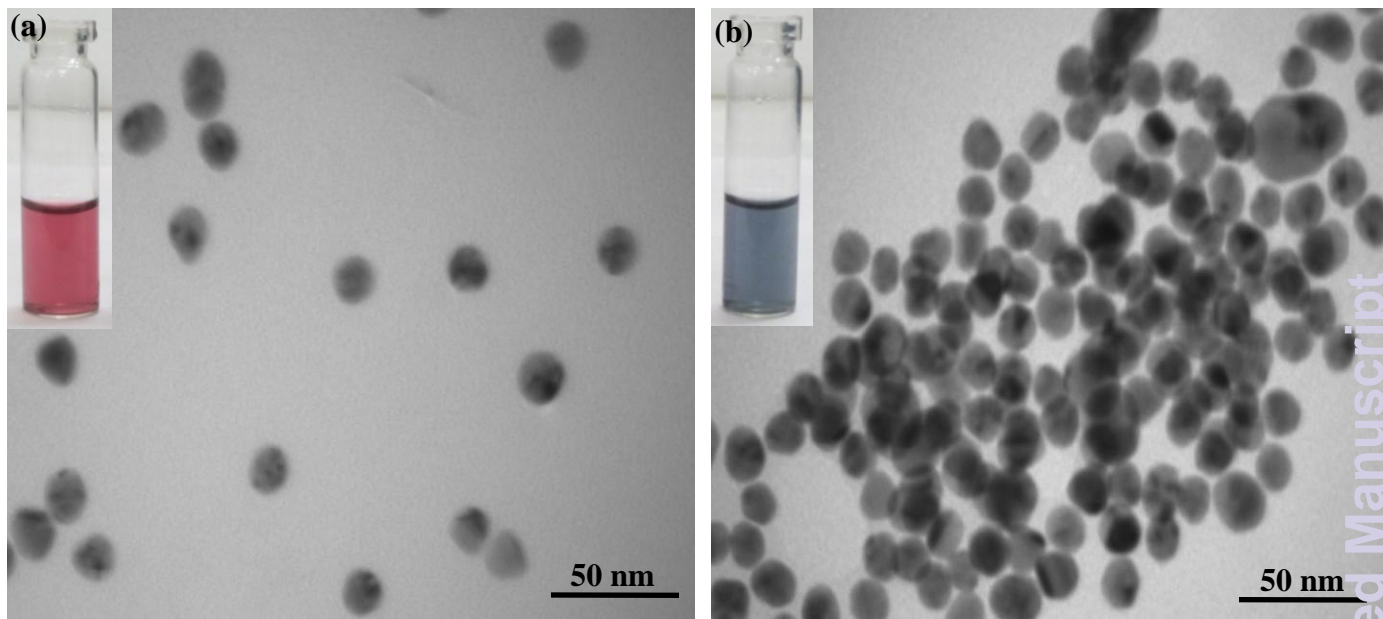


Figure 3

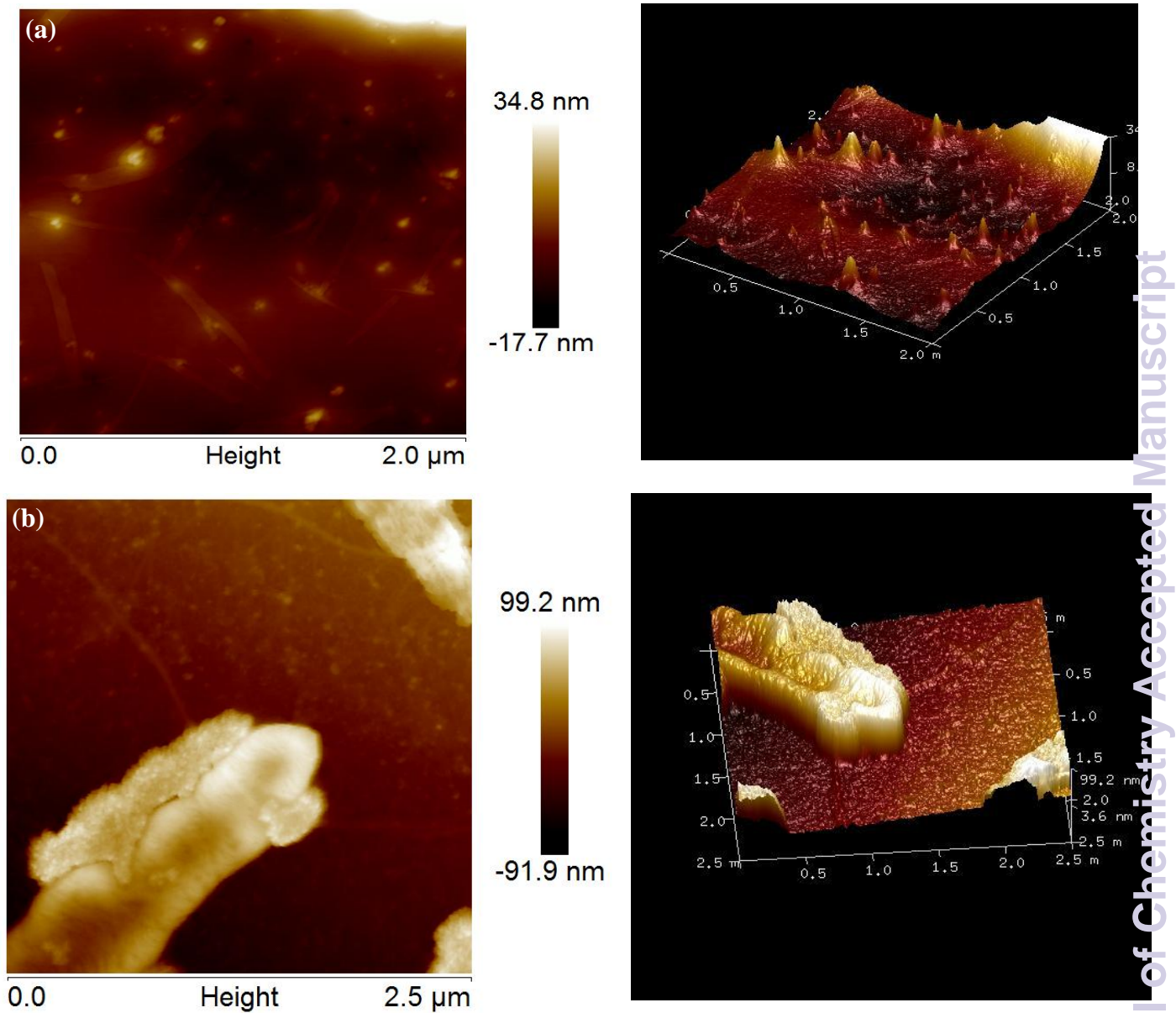


Figure 4

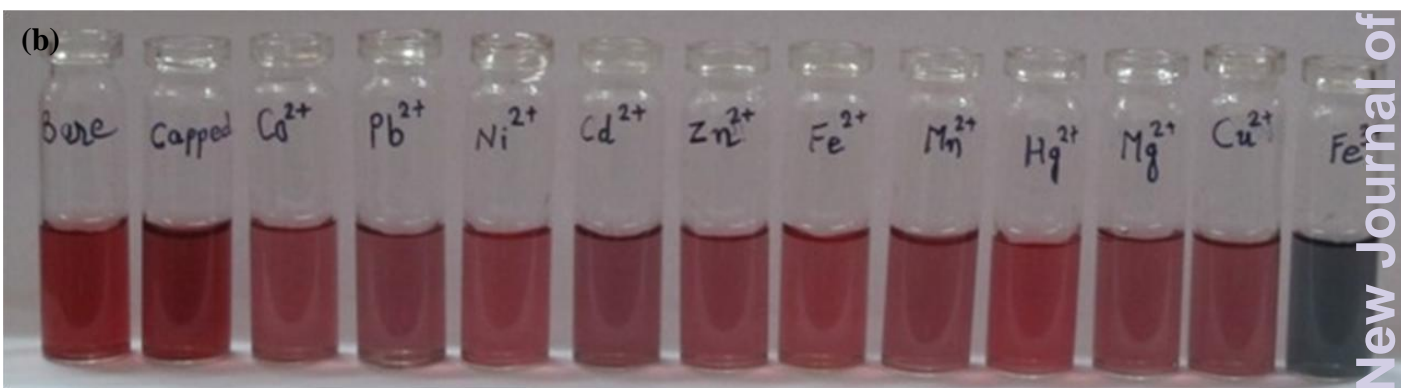
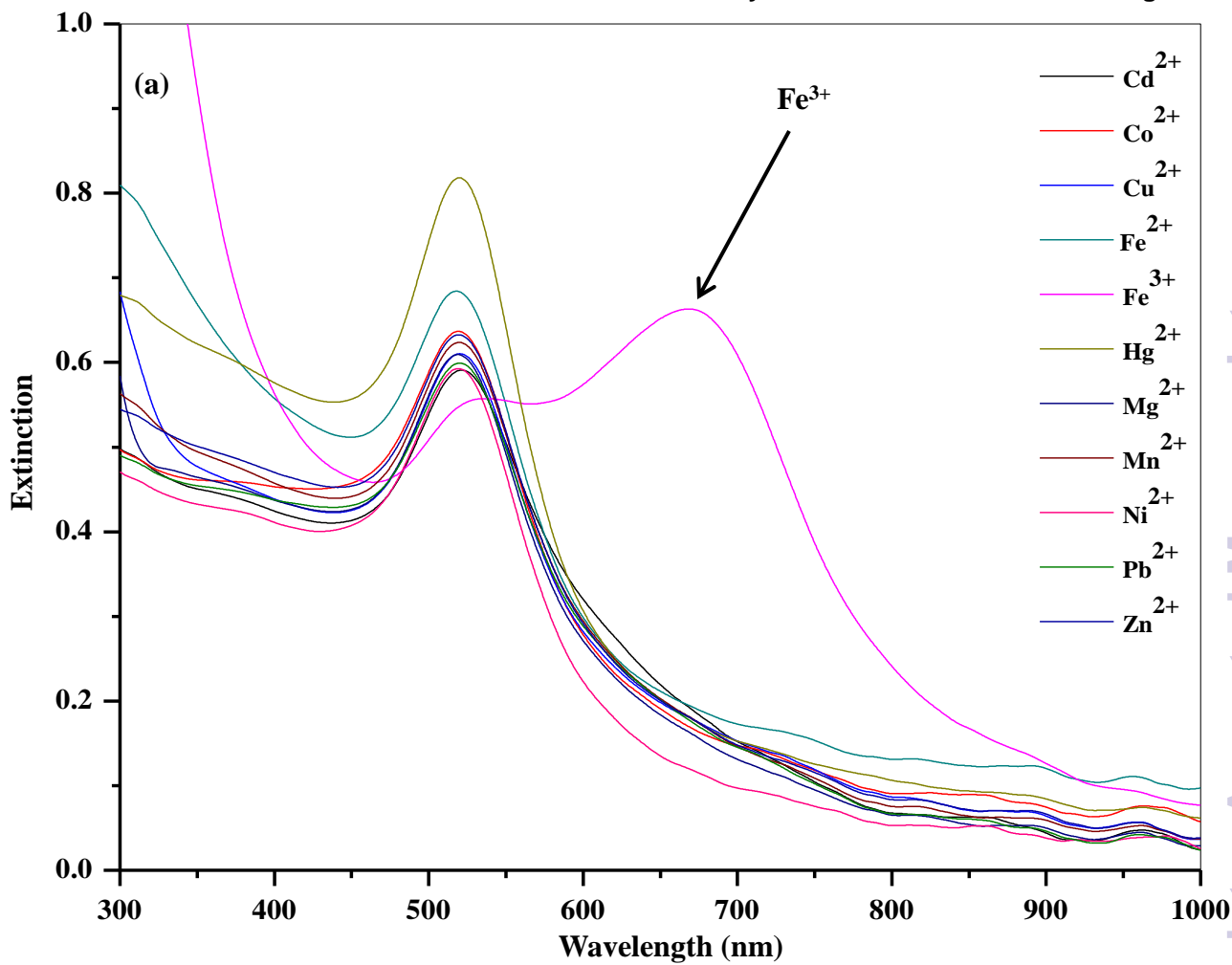


Figure 5

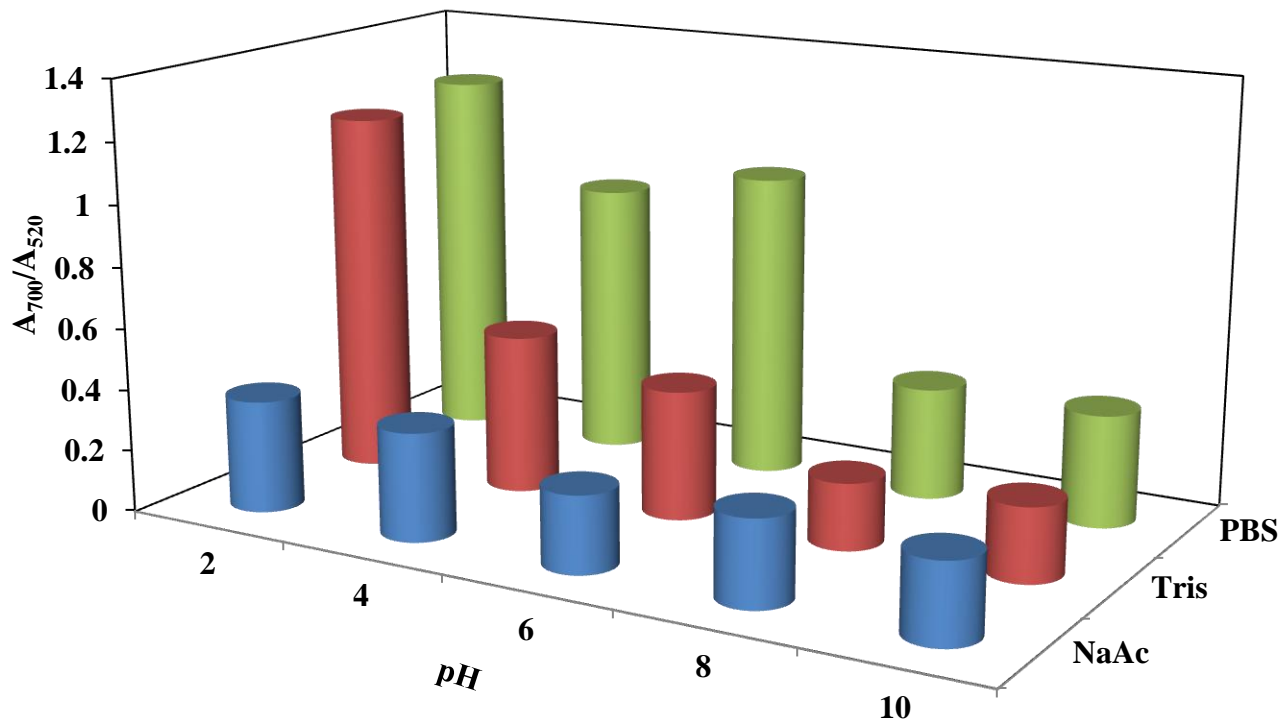


Figure 6

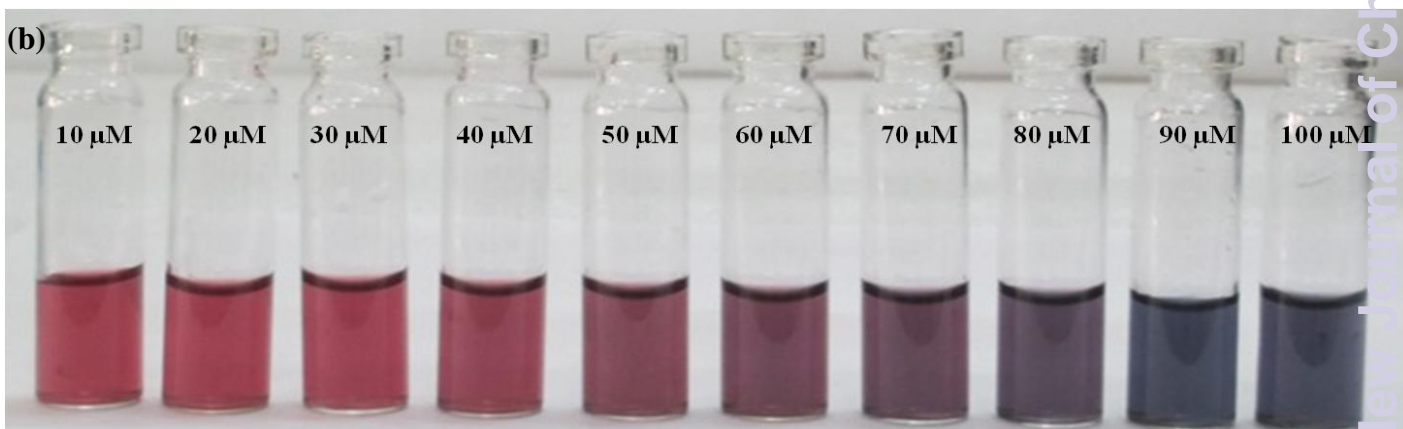
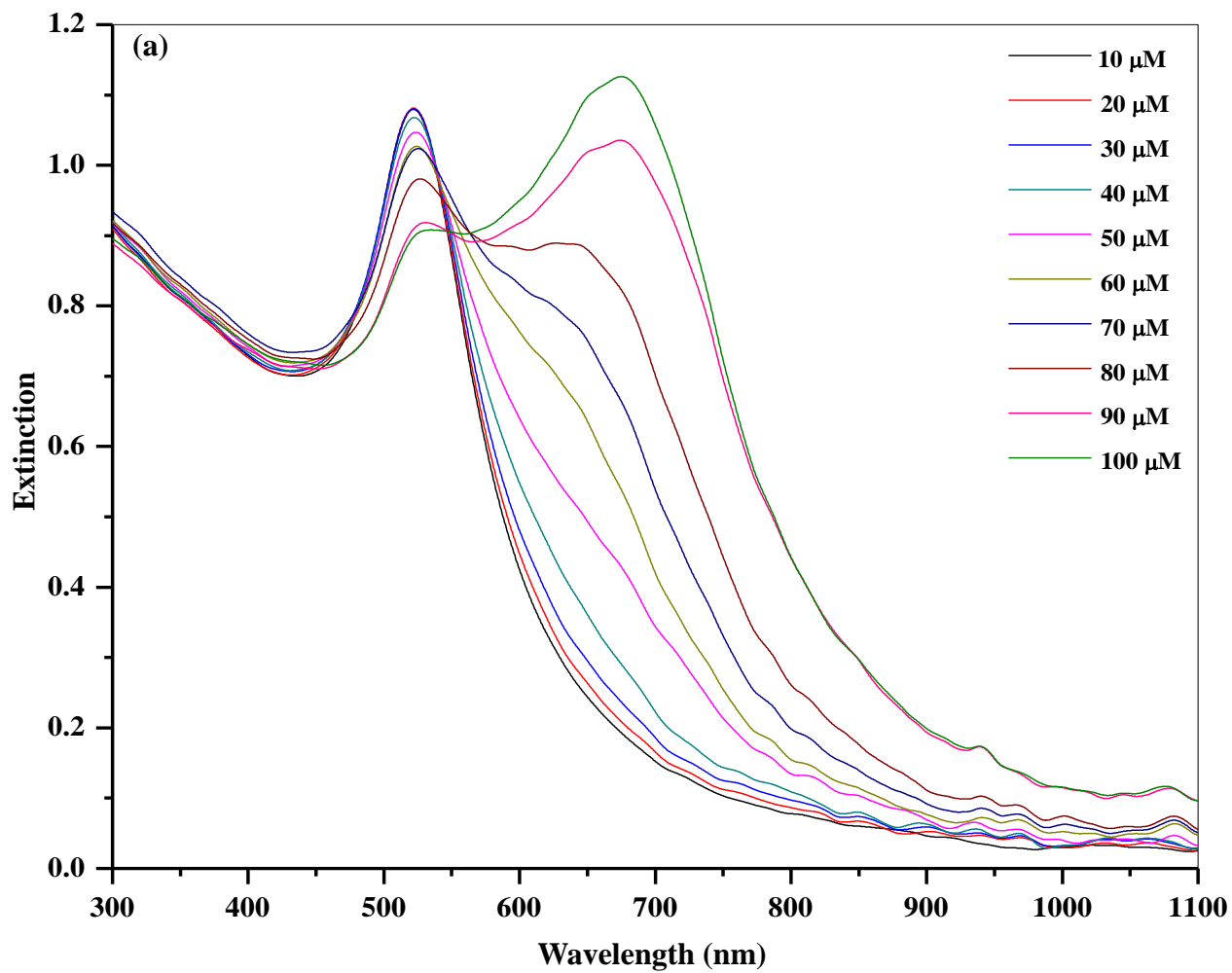


Figure 7

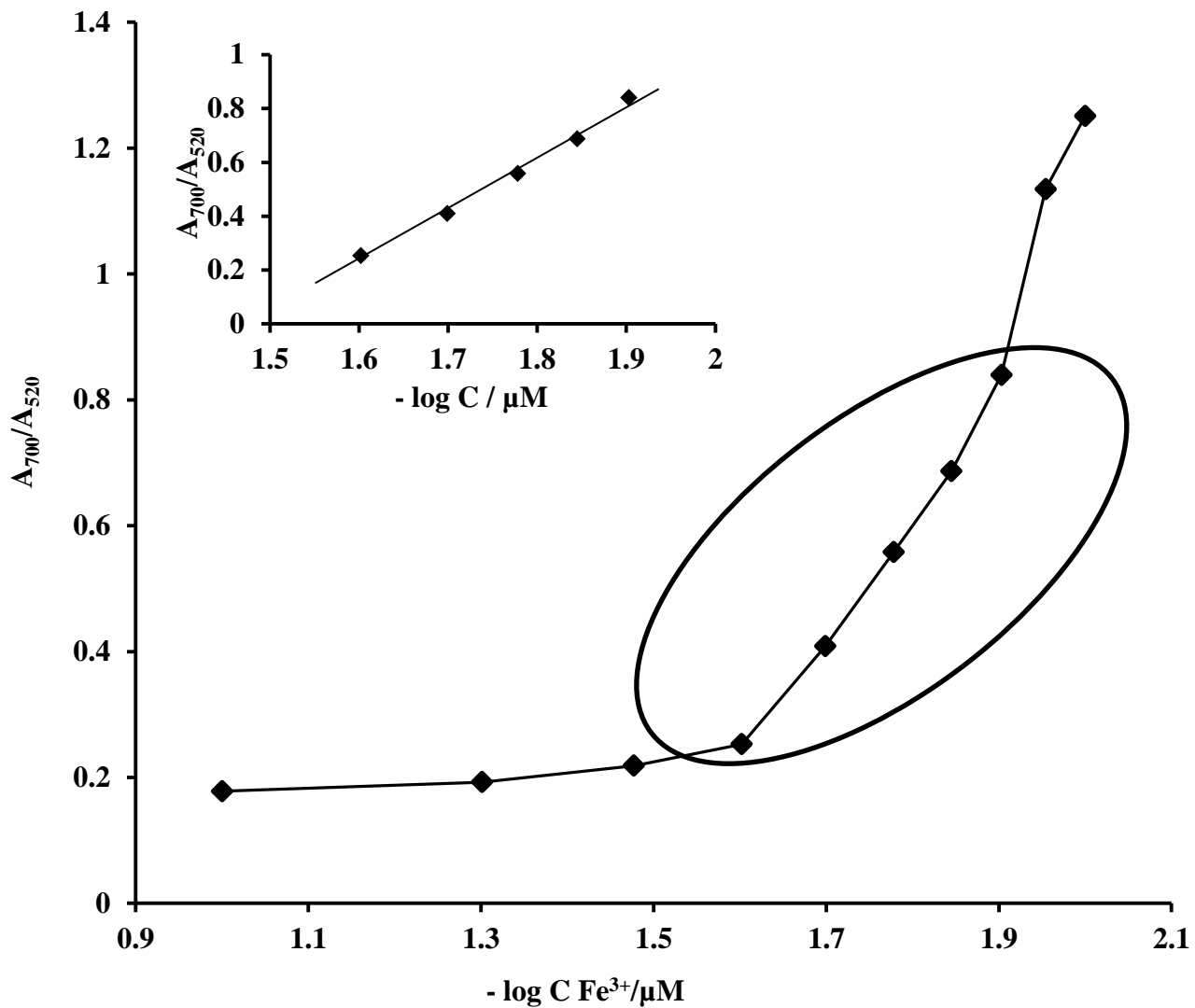


Figure 8